Polycaprolactone and polycaprolactone/chitosan nanofibres functionalised with the pH-sensitive dye Nitrazine Yellow, L. Van der Schueren, T. De Meyer, I. Steyaert, O. Ceylan, K. Hemelsoet, V. Van Speybroeck, K. De Clerck, Carbohydrate Polymers , 91 (1), 284-293 , 2013
http://dx.doi.org/10.1016/j.carbpol.2012.08.003

Highlights

- pH-sensitive PCL and PCL/chitosan nanofibres are successfully electrospun.
- pH-sensitive PCL and PCL/chitosan nanofibres show a clear halochromic response.
- Chitosan addition results in a significantly increased water sorption.
- Chitosan addition is indispensable for a sensitive and rapid response.
- Theoretical modelling on the dye-polymer interactions underpins the experimental findings.

Polycaprolactone and polycaprolactone/chitosan nanofibres functionalised with pH-sensitive dyes

Lien Van der Schueren[1]
lien.vanderschueren@ugent.be

Thierry De Meyer[1,2]
thierry.demeyer@ugent.be

Iline Steyaert[1]
iline.steyaert@ugent.be

Özgür Ceylan[1]
ozgur.ceylan@ugent.be

Karen Hemelsoet[2],
karen.hemelsoet@ugent.be

Veronique Van Speybroeck[2]
veronique.vanspeybroeck@ugent.be

Karen De Clerck[1*]
karen.declerck@ugent.be
T +32 9 264 57 40
F +32 9 264 58 46

[1] Ghent University, Department of Textiles
Technologiepark 907, 9052 Zwijnaarde (Ghent), Belgium

[2] Ghent University, Center for Molecular Modeling
Technologiepark 903, 9052 Zwijnaarde (Ghent), Belgium

Abstract

Nanofibres functionalised with pH-sensitive dyes could greatly contribute to the development of stimuli-responsive materials. However, the application of biocompatible polymers is vital to allow for their use in (bio)medical applications. Therefore, this paper focuses on the development and characterisation of pH-sensitive polycaprolactone (PCL) and PCL/chitosan nanofibrous structures. Electrospinning with added pH-sensitive dyes proved to be an excellent method resulting in functionalised non-wovens. Unlike the slow and broad response of PCL nanofibres, the use of blends with chitosan led to an increased sensitivity and significantly reduced response time. These important effects are attributed to the increased hydrophilic nature of the nanofibres containing chitosan. Computational calculations underpinned our experimental observations indicating different interactions of the dye with PCL and chitosan polymeric chains. In conclusion, because of the unique characteristics of chitosan, the use of PCL/chitosan blends in pH-sensitive biocompatible nanofibrous sensors is crucial.

Keywords chitosan, polycaprolactone, nanofiber, hydrophilicity, pH-sensitive, sensor

1. Introduction

Polycaprolactone (PCL) is an aliphatic polyester, often used in (bio)medical applications because of its biocompatibility, slow biodegradability, low-cost, non-toxicity and good mechanical properties (Moghe et al., 2009; Van der Schueren et al., 2011). However, PCL is hydrophobic (Prabhakaran et al., 2008) which may severely limit the use of PCL in certain applications. Combining PCL with the natural polysaccharide chitosan, derived from chitin, might significantly improve its material characteristics. Chitosan indeed provides hydrophilicity and antimicrobial activity and, moreover, supports the biocompatibility of PCL (Prabhakaran et al., 2008; Yang et al., 2009; Bhattarai et al., 2009; Hong & Kim, 2011; Cooper et al., 2011). The combination of PCL with the carbohydrate polymer chitosan may thus be greatly relevant and contribute to the development of innovative materials.

Stimuli-responsive polymeric materials belong to a rapidly evolving field of research (Stuart et al., 2010). Within textiles, the research towards chromic fibrous materials is of particular

value (Matilla et al., 2006; Little & Christie, 2005). These materials, which reversibly change colour due to an external stimulus, are prime candidates for sensor systems because of their simplicity and flexibility. Halochromic or pH-sensitive textiles, even though so far less exploited, offer major potential within these chromic materials. Numerous possible applications for pH-sensitive textiles exist including protective clothing, filtration, wound dressings etc (Van der Schueren et al., 2012a). Yet, for future practice, also the choice of polymer type is essential to address as this may greatly influence the functioning of the obtained materials (Lloyd et al., 1998).

Because of the small diameter of nanofibres, nanofibrous structures show unique characteristics such as small pore sizes, high porosity, high specific surface area and high absorbance capacity (Ramakrishna et al., 2005). The latter properties render them highly suited to be used in chromic sensors. A nanofibrous structure may increase the sensitivity and reduce the response time, both being important demands for sensor systems. Moreover, nanofibres are widely known to promote healing of damaged tissue and are thus believed to be ideal wound dressing materials (Greiner & Wendorff, 2007). However, thus far, only little research has been performed on chromic nanofibres. Nevertheless, recent studies on thermochromic and photochromic nanofibres establish the favourable, intrinsic benefits of nanofibrous structures for sensor applications (Fengyu et al., 2009; Mao et al., 2009; Liu et al., 2010; Malherbe et al., 2010) . Moreover, our previous study on halochromic polyamide nanofibres proved the potential of pH-responsive nano systems (Van der Schueren et al., 2010b). Though, the studied polyamides show limitations for use in (bio)medical applications. As a consequence, further research towards pH-sensitive biocompatible nanofibres is key to fully exploit their potential. PCL can contribute to this development but its hydrophobic nature may need to be tackled since it may impact the sensor properties. The important effect of the speed of sample wetting on the resulting time lag of the sensor has indeed been demonstrated (Van der Schueren et al., 2010a; Van der Schueren et al., 2010b). Therefore, the addition of chitosan is studied as a potential solution for this hydrophobic nature.

The aimed blend nanofibres of PCL and chitosan can be successfully obtained via electrospinning a blend polymer solution (Van der Schueren et al., 2012b). This paper thus discusses the development of pH-sensitive PCL and PCL/chitosan nanofibres via electrospinning. Nitrazine Yellow (NY) is selected as pH-sensitive dye as it is proven to be

successful on polyamide nanofibres (Van der Schueren et al., 2012c). The functionalisation of the nanofibres can be realised by adding the pH-sensitive agent to the polymer solutions, prior to the electrospinning process. The influence of this dye addition on the electrospinning and fibre morphology is to be examined followed by an analysis of possible dye leaching. The halochromic behaviour of the nanofibres is studied based on spectroscopic measurements.

To validate the experimental results and to understand the nature of the interactions between dyes and nanofibres, molecular modelling is applied. Recently, theoretical considerations have been used to study the colour changing mechanism of azo dyes (De Meyer et al., 2012; Jacquemin et al., 2010; Teimouri et al., 2009). With the fast evolution of computational protocols it is now also possible to study the effect of molecular environment (Catak et al., 2010; Catak et al., 2011). Moreover, molecular modelling showed to be promising for studying interactions between molecules (Gu et al., 2008). This innovative approach may lead to a greater understanding of the interaction of dye molecules with the polymer matrix on a molecular level, deepening the understanding of the influence of dye-polymer interactions on the halochromic behaviour of dyes.

In conclusion, the main objective of this paper is to study pH-sensitive PCL and PCL/chitosan blend nanofibrous structures and to compare their performance. The results obtained in this paper will greatly contribute to the development of innovative textile sensors ideally suited for medical applications and will, moreover, highlight the positive impact of chitosan on the characteristics of synthetic polymers in general.

2. Materials and Methods

2.1 Materials

Medium molecular weight chitosan and PCL (M_n 70,000-90,000) were supplied by Sigma Aldrich. Also the solvents 98 v% formic acid and 99.8 v% acetic acid, Nitrazine Yellow (NY), hydrochloric acid, sodium hydroxide and potassium nitrate were supplied by Sigma Aldrich. The complexing agent poly(diallyldimethylammonium chloride) (Perfixan RDV) was kindly supplied by Chemotex (Kortrijk, Belgium).

2.2 Preparation and characterisation of the electrospinning solutions

The 14 wt% PCL electrospinning solutions were prepared in a 1:9 acetic acid-formic acid solvent system as this system results in reproducible nanofibres with a small fibre diameter distribution (Van der Schueren et al., 2011). For the PCL/chitosan blend nanofibres, a polymer blend containing 6 wt% PCL and 20 % chitosan in 3:7 acetic acid-formic acid was chosen since this allows for reproducible nanofibres with a considerable amount of chitosan (Van der Schueren et al., 2012b). A certain amount of NY, expressed in % on mass of fibre (% omf) was added to the polymer solutions. The solutions were magnetically stirred at room temperature for three-and-a-half hours, time needed for complete dissolution. The viscosity of the solutions obtained was measured using a Brookfield viscometer LVDV-II. The conductivity was measured with a CDM210 conductivity meter (Radiometer Analytical).

2.3 Electrospinning of PCL and PCL/chitosan nanofibres

During the electrospinning process, the polymer solutions were pumped from a 20 ml syringe into a 15.24 cm long needle with an inner diameter of 1.024 mm. A KD Scientific Syringe Pump Series 100 regulated the flow rate of the solution. The voltage was adjusted using a Glassman High Voltage Series EH 30P3 source (voltage range 0 to 30 kV). Electrospinning was carried out at room temperature (22 ± 2 °C) and a relative humidity of 40 ± 5 %. The tip to collector distance was set at 12.5 cm. To electrospin PCL, the flow rate was set at 1 ml h^{-1} while this was 0.6 ml h^{-1} for electrospinning the polymer blend.

2.4 Characterisation of electrospun samples

The morphology of the electrospun structures was examined using a Scanning Electron Microscope (SEM) (FEI QUANTA 200 F). Prior to SEM-measurements, the sample was coated with gold using a sputter coater (Balzers Union SCD 030). Fifty diameter measurements on each sample using Cell D software (Olympus) determined the average fibre diameter.

Contact angle measurements were carried out with the drop-shape analysis system DSA 10-Mk2, coupled to a control unit G120 Mk1/G140-Mk1 and with the drop-shape analysis software DSA1 (v1.80, Krüss).

Dynamic Vapour Sorption (DVS) measurements were conducted in a Q-5000SA instrument (TA-instruments, Zellik, Belgium). All measurements were performed at 23 °C ± 0.1 °C. Deliquescent salts (sodium bromide and potassium chloride) were used to verify the humidity of the instrument. 4 mg of nanofibres were placed in the quartz sample pans. At the start of each moisture sorption cycle, the fibres were dried at 0 % relative humidity (RH) until the weight change was stabilised to be less than 0.05 % for a period of 15 minutes. After the stabilisation, the moisture sorption cycle was started and the humidity was increased stepwise, with steps of 10 % RH from 5 % till 95 %. At every RH, the equilibrium moisture concentration is monitored after reaching equilibrium, or thus when the weight change is less than 0.05 % over a time period of 15 minutes.

Dye leaching of the electrospun samples was analysed by placing 0.012 g of the nanofibrous samples in 10 ml of demineralised water at pH 8. After 24 hours the absorbance of the water solution with possible released dye was measured by UV-Vis spectroscopy and finally the dye release was converted into percentage release with respect to the original amount of dye present in the samples.

2.5 Characterisation of halochromic behaviour

The halochromic behaviour of the samples was analysed by immersing them into aqueous pH baths. pH measurements were executed with a combined reference and glass electrode (SympHony Meters VMR). Potassium nitrate with a concentration of 10^{-2} mol l^{-1} was added to ensure a constant activity coefficient during measurements. Hydrochloric acid and sodium hydroxide were used to adjust the pH.

The UV-Vis spectra were recorded with a Perkin-Elmer Lambda 900 spectrophotometer. For the transmission spectra of solutions 1 cm matched quartz cells were used, for the reflection measurements on fabrics an integrated sphere (Spectralon Labsphere 150 mm) was used. The spectra were recorded from 380 nm to 780 nm with a data interval of 1 nm (transmission) and 4 nm (reflection). The resulting absorbance (for solutions) and Kubelka-Munk (for fabrics) spectra were normalised to a value of one at the peak maximum to account for possible artefacts due to dye leaching for some of the samples.

2.6 Computational details

The use of Density Functional Theory (DFT) provides a valid compromise between computational resources and chemical accuracy. All computations in this work were carried out in the Gaussian09 software package, using the M06-2X electronic structure method in combination with a 6-311G(d,p) basis set (Frisch et al., 2009; Zhao et al., 2008). The DFT-functional M06-2X is a meta hybrid high-nonlocality functional with double the amount of non-local exchange (2X), which has proven to be a good method to model systems where dispersion interactions are important (Gu et al., 2008; Catak et al., 2010; Catak et al., 2011; Zhao et al., 2008). Frequency calculations were performed at the same level of theory as the geometry optimisation to validate that all points are true minima on the potential energy surface and to obtain the necessary temperature corrections of the Gibbs free energies.

3. Results and Discussion

3.1 Electrospinning of pH-sensitive PCL and PCL/chitosan nanofibrous structures

Adding components to the electrospinning solutions might significantly affect the solution parameters and thus the electrospinning process (Li & Xia, 2004). Therefore, different amounts of NY were added to the polymer solutions after which the viscosity and conductivity were determined. Moreover, also poly(diallyldimethylammonium chloride) was added as dye complexing agent since preliminary experiments established the need of its addition to avoid dye leaching. The viscosity of the solutions was not significantly influenced by the addition of the components. The viscosity was on average 2667 mPa.s for the PCL solutions and 7188 mPa.s for the PCL/chitosan solutions. In contrast to the viscosity, the conductivity was affected by the dye addition, the effect being more prominent for pure PCL solutions (Table 1). The conductivity increases with increasing NY concentration for both polymer systems due to the charges brought into the solution by the dye molecules. However, because of the polycationic nature of chitosan, the intrinsic conductivity of the blend polymer solutions is much higher compared to the pure PCL solutions and their conductivity is thus less influenced by the dye addition. Also the complexing agent has an effect on the conductivity of PCL and PCL/chitosan solutions, the influence being again less pronounced for the polymer blend. The complexing agent is indeed a polycationic molecule, increasing the solution's conductivity.

All solutions stated in Table 1 could be successfully electrospun using the parameters stated in the Materials and Methods section. The stability of the electrospinning process was not affected by the addition of NY, nor by the addition of the complexing agent. All PCL solutions were electrospun at an applied voltage of 18 kV while this was 26 kV for the PCL/chitosan blend nanofibres. Thus, despite the distinct variation in solution's conductivity, the electrospinning process itself remained unaffected. This agrees well with our previous study on pH-sensitive polyamide nanofibres which reported that the electrospinning process was not influenced in case of well dissolved dyes (Van der Schueren et al., 2010b). The results hence indicate that electrospinning with added components is an adequate method giving functionalised PCL and PCL/chitosan nanofibres. Next, the characterisation of the nanofibrous samples is discussed.

3.2 Characterisation of pH-sensitive PCL and PCL/chitosan nanofibrous structures

The fibre morphology of the electrospun samples with added pH-sensitive dye was similar to the morphology of reference blank nanofibrous structures as demonstrated by the SEM images in Fig. 1. A uniform, beadless non-woven was obtained at each dye concentration. In addition, the PCL/chitosan blends all showed an ultrafine nanofibrous web formed in between the main fibres while this web was not present in PCL nanofibrous structures. This phenomenon is attributed to the presence of chitosan (De Vrieze et al., 2007; Geng et al., 2005; Nirmala et al., 2011, Van der Schueren et al., 2012c) and the added components thus did not affect the ultrafine web formation. Moreover, the average fibre diameters of PCL and PCL/chitosan nanofibres (Table 1) indicate that the diameter is not significantly influenced by the addition of NY, nor by the addition of the complexing agent. These results underpin the thesis that the electrospinning process and its stability do not alter after the addition of NY and the complexing agent to PCL and PCL/chitosan solutions. Yet, a pronounced diameter decrease was noticed for the PCL/chitosan blend nanofibres compared to the PCL nanofibres, consistent with literature (Shalumon et al., 2010; Van der Schueren et al., 2012b).

After characterisation of the fibre morphology, the hydrophilic nature of the PCL and PCL/chitosan samples was examined. Contact angle measurements, being a useful indicator of wettability of substrates, showed a decrease in contact angle from 129° for PCL to 120° for PCL/chitosan nanofibres. This thus already shows a higher hydrophilicity for the chitosan

blend. Moreover, the contact angle of PCL nanofibres remained constant during 20 seconds after droplet formation while the angle of PCL/chitosan nanofibres decreased to 116° after 20 seconds. Hence, the blend nanofibres absorb water more efficiently. To support this theory, DVS experiments were carried out. DVS is a well-suited technique to study the moisture sorption of a compound (Markova et al., 2001) and is thus applied to study the moisture sorption of the nanofibrous structures. A clear difference between both samples was found as demonstrated in Fig. 2. The PCL/chitosan structures absorb more water, resulting in a greater weight change (5.6 % weight change compared to 0.9 % for PCL at 95 % RH). Moreover, adsorption isotherms are classified in five types according to the IUPAC classification. Type II and III describe adsorption on macroporous and non-porous adsorbents with strong and weak adsorbate-adsorbent interactions respectively (Sangwichien et al., 2002). With the presence of chitosan, the shape of the curve changes from a rather type III-isotherm to a rather type II-isotherm as seen in Fig. 2. Thus, also the shape of the isotherms strongly suggests an increased interaction with water when chitosan blend nanofibres are used.

As a final step prior to the halochromic study, the dye leaching of the samples is characterised (Table 1), following the procedure explained in Materials and Methods. A clear difference between dye leaching of PCL and PCL/chitosan samples with 0.5 % omf NY was noticed (4.8 % for PCL and 57.1 % for PCL/chitosan). The relatively low dye release of the PCL nanofibrous structures is probably attributed to a combined effect of the material's hydrophobicity and an interaction between PCL and NY. Due to the hydrophobic nature of PCL, the samples are hardly wetted, minimizing contact between water and NY molecules and hence dye leaching. To increase the wettability, addition of chitosan is vital as shown in Fig. 2. However, owing to the increased hydrophilicity, the dye release increases as well. Therefore, a dye complexing agent was added resulting in a decreased dye release for both PCL and PCL/chitosan. Samples with 0.25 and 0.5 % omf NY and 4 % omf complexing agent did not show any dye release. These data demonstrate the promising potential of PCL and PCL/chitosan pH-sensitive nanofibres and prove the need of the complexing agent addition to avoid dye leaching of the blend nanofibres.

3.3 Halochromic behaviour of pH-sensitive PCL and PCL/chitosan nanofibrous structures

The nanofibrous samples were all yellow just after the electrospinning process, in agreement with the acidic conditions during their production (acetic acid-formic acid solvent system). However, after conditioning the samples during 24 h in a neutral air atmosphere, their visual aspect showed a clear variation. The PCL nanofibrous structure only containing NY remained yellow while the PCL samples with the addition of complexing agent changed to green. On the other hand, all PCL/chitosan nanofibres obtained a blue colour, in agreement with the colour of a neutral aqueous NY solution.

Even after immersion in a strongly alkaline pH bath (pH 11), the PCL sample with only NY did not present a colour shift whereas the PCL/chitosan samples as well as the PCL sample with complexing agent showed a clear shift to a blue colour. This may be caused by interactions between PCL and NY blocking the halochromic transition from the protonated to the deprotonated molecule, which is known to be responsible for the halochromism of the dye (Van der Schueren et al., 2012c). By contrast, chitosan and the complexing agent may interact differently with NY, still allowing for the halochromic transition. To underpin these theories, molecular modelling was performed and will be discussed in a later section.

Since PCL samples with only NY do not show a halochromic response and PCL/chitosan samples with NY suffer from a high dye release (Table 1), the discussion on the halochromic behaviour further focuses on the samples to which the complexing agent is added. The PCL nanofibrous samples showed a reversible colour transition from yellow over green to blue. The analysis of the colour was performed after immersion of the samples during 3 h in the pH baths, time during which the colour of the immersed nanofibres still changed. The time lag for the halochromic transition of the PCL nanofibrous structures was thus large limiting the practical use of these PCL sensor systems. Similar to the colour transition of PCL nanofibres, PCL/chitosan structures reversibly altered from yellow to blue with a variation in pH. However, the time lag for this halochromic response was 5 min at maximum, this being greatly shorter than the time needed for the pure PCL samples. This rapid response is caused by the increased hydrophilicity of the blend nanofibres resulting in a fast wetting of the entire nanofibrous structure. Chitosan addition is thus of utmost importance for obtaining a fast sensor system.

To study the effect of dye concentration, the halochromic response was recorded for three different NY concentrations being 0.25, 0.5 and 1 % omf NY. The dynamic pH range of PCL

structures was found to broaden with increasing dye concentration. This is demonstrated in Fig. 3b which depicts the variation in normalised Kubelka-Munk value at the acidic and alkaline peak maximum as a function of pH. This observation agrees well with previous literature on polyamide nanofibrous structures (Van der Schueren et al., 2012c) and is most likely related to accessibility issues. Owing to the highly hydrophobic nature of PCL (section 3.2), the NY molecules are difficult to access, leading to a slow and broad response. Indeed, compared to the sharp transition of NY in aqueous solutions, which occurs between pH 6 and 8 (Fig. 3a), the response of PCL nanofibres is less sensitive (response between pH 4 and 10, Fig. 3b). Moreover, besides alterations to the pH range, also the wavelength maxima depend on the NY concentration, again most likely caused by the low water sorption of the samples and hence the different accessibility. The acidic maximum decreases from 474 nm at 0.25 % omf NY to 464 nm at 1 % omf NY, the alkaline maximum increases from 606 nm at 0.25 % omf to 612 nm at 1% omf. In addition, these wavelength maxima differ from the maxima found for NY in solution (466 nm and 590 nm), consistent with numerous studies on the behaviour of dyes in different environments (Ertekin et al., 2003; Garcia-Heras et al., 2005; Jurmanovic et al., 2010; Van der Schueren et al., 2012a). Indeed, due to the interactions between NY and the surrounding polymeric matrix, changes to the dye characteristics are very likely.

The augmented hydrophilicity of PCL/chitosan blends led to an easy accessibility of all dye molecules, even at higher NY concentrations. Due to this effect, no differences in halochromic behaviour with varying NY concentration (0.25, 0.5 and 1 % omf NY) were observed. All PCL/chitosan samples showed a sharp transition between pH 4 and 6 (Fig. 3c). Also the wavelength maxima did not alter and remained constant at 474 nm and 605 nm in acidic and alkaline environment respectively. Yet, even although no influence of the dye concentration was observed, the halochromism of PCL/chitosan nanofibres differs from the behaviour of NY in solution. Due to interactions between the dye and chitosan, the dynamic pH range, albeit similarly sharp, underwent an acidic shift of two pH units after incorporation in the polymeric blend. The effective halochromic behaviour of PCL/chitosan nanofibres loaded with NY establishes their major potential to be used as fast and sensitive sensor systems in the slightly acidic pH range.

As a final step of the halochromic study, the colour of the nanofibrous structures after 24 h immersion in the pH baths was analysed. No change in colour was observed for the

PCL/chitosan samples confirming that all present dye molecules almost immediately assumed their final conformation. The PCL samples, however, did show a further colour change. This is clearly demonstrated in Fig. 4 showing the spectra of PCL nanofibres with 0.5 % omf NY at pH 6 recorded after 3 and 24 h. While the dominant peak after 3 h immersion was at 470 nm (the acidic maximum), it is shifted to 607 nm (the alkaline maximum) after 24 h immersion and only a small peak at 470 nm remained. A higher resemblance to the spectrum of PCL/chitosan was hence obtained. Eventually this further colour change resulted in a sharper dynamic pH range after 24 h immersion, Fig. 3d. The low dye concentration (0.25 % omf) almost coincides with the graph obtained with PCL/chitosan (Fig. 3c) while also the highest concentration (1 % omf) shows a narrower pH range compared to the results after 3 h, even though it is still broader. A long immersion time, dependent on the dye concentration, is thus necessary to allow for a complete conversion of all NY molecules in PCL nanofibres because of their slow wetting. These results underpin the fact that the differences found between PCL and PCL/chitosan nanofibres loaded with the complexing agent are mainly attributable to their different water sorption characteristics. In conclusion, the presence of chitosan is vital as to obtain an adequate sensor with a rapid response.

3.4 Interpretation of halochromic behaviour using molecular modelling

In this section, molecular modelling is used to gain molecular-scale insight into the difference in halochromic behaviour of NY incorporated in PCL and PCL/chitosan. Focus is given to the pure polymers, thus omitting the complexing agent from the discussion. First, a hypothesis of the possible interactions of NY with the different polymeric chains will be proposed, which will then be validated by theoretical results.

In Fig. 5, the chemical formulas of the molecules relevant to this discussion are displayed. As discussed in previous work (Van der Schueren et al., 2012c), the halochromism of NY (Fig. 5a) arises from the removal of the hydrogen atom bonded to the azo group by the alkaline solvent.

After electrospinning pure PCL (Fig. 5b) with NY, no halochromic behaviour is observed, which is an indication of an interaction of PCL with NY that screens NY from possible interactions with the water solvent. When inspecting the chemical formulas, an interaction of the PCL ester group with the NY azo group seems most plausible, meaning that the hydrogen

atom remains bonded to the azo group and hence no colour change can occur. In combination with the hydrophobic properties of PCL, this can explain the loss of pH-sensitive behaviour of NY when interacting with PCL. In case of chitosan (Fig. 5c), an interaction of the amino groups with the sulphate groups of NY is feasible. If this interaction turns out to be stronger than the interaction of NY with PCL, NY will almost solely interact with chitosan in the PCL/chitosan blend. Chitosan is, in contrast to PCL, a hydrophilic fibre. Water molecules can thus easily penetrate into the fibre matrix and can reach the NY molecules. If previous hypothesis is correct, the azo group is not directly involved in the interaction between PCL and the chitosan fibres, and remains accessible for water molecules. Incorporated in chitosan, NY is thus still susceptible to deprotonation in alkaline environment and can hence show halochromic behaviour.

To validate the previous assumptions, molecular modelling calculations were performed on the dye and polymeric chains in order to obtain profound insight into the interactions and associated energies. The sodium ions are omitted from the calculations, as was previously validated to be a good model (De Meyer et al., 2012). For both PCL and chitosan a valid model system was constructed which allows to represent the most essential interactions (Fig. 5d and 5e). In case of PCL one ester group terminated by two n-propyl groups is taken into account. For chitosan a dimeric model was used consisting of two monomeric units which are terminated by methyl groups. Such a dimeric system has already shown to be a good model for chitosan (Braier et al., 2000). Proton affinities (PA) were calculated for both model structures. The chitosan model (Fig. 5e) has a PA of 908 kJ/mol, which is much higher than the value of 841 kJ/mol obtained for the PCL model (Fig. 5d). This suggests that the chitosan amino groups get preferentially protonated to NH_3^+ in acidic circumstances. Optimised structures of NY interacting with the PCL and chitosan model systems are shown in Fig. 6 and 7.

Several interaction patterns of the NY-PCL complex were explored, including hydrogen bonding of the PCL ester group oxygen with the NY hydrogen atom on the NY azo bond, but the geometry depicted in Fig. 6 was found to be most optimal. The corresponding interaction Gibbs free energy (ΔG_{298}) was found to be -35.6 kJ/mol. The expected interactions are indeed present; the ester group interacts via long range interactions with the chromophoric unit, thus shielding the halochromic group from any interaction with water molecules. This interaction energy is also high enough to explain the low value for dye leaching, especially when

combined with the hydrophobic properties of PCL. The ΔG-value in the case of chitosan (Fig. 7) is much higher, -132.3 kJ/mol. The value for dye leaching was, however, much larger in this case, which is probably because of the hydrophilic properties of chitosan. As seen from Fig. 7, the interaction is a combination of electrostatic interactions between the sulphate groups of NY and the amino groups of chitosan and hydrogen bonds. The high interaction value indicates that NY preferentially interacts with chitosan. In this conformation, in line with the aforementioned assumptions, the halochromic group is still accessible for water, thus maintaining halochromic behaviour. The complexing agent used in this work is a polycationic chain. The same ionic bound with NY as in the case of chitosan can therefore be expected, leading to the halochromic response of PCL nanofibres to which not only NY but also the complexing agent is added.

The molecular modeling calculations help to reveal the essential nature of the interactions and to understand the experimental observations. This knowledge leads to a better understanding of halochromic behaviour in terms of the environment and can eventually lead to a better application of halochromic dyes in the future.

4. Conclusion

In this paper, PCL and PCL/chitosan nanofibrous structures loaded with the pH-sensitive dye NY were investigated as possible biocompatible sensor systems. The pH-sensitive nanofibres could be successfully obtained using the electrospinning technique. To minimize dye leaching, addition of a complexing agent was recommended. The morphology of the functionalised nanofibres was similar to the morphology of blank PCL and PCL/chitosan nanofibres.

Molecular modelling strongly suggested a different interaction of NY with PCL and chitosan polymeric chains. While the interaction with PCL shields the group responsible for the pH-sensitive behaviour, the interaction with chitosan – being stronger than the interaction with PCL – still allows for a halochromic response. Owing to a similar ionic interaction, the addition of the complexing agent also led to a pH-sensitive PCL nanofibrous structure.

The obtained PCL and PCL/chitosan nanofibres (with addition of complexing agent) showed a reversible halochromic transition, but significant differences between both polymeric

systems were found. While a slow response was observed for the PCL structures, the PCL/chitosan samples demonstrated a rapid halochromic response. Moreover, the transition occurred in a sharp pH range from pH 4 to 6 for the PCL/chitosan nanofibres while a broad pH range was noticed for PCL. The increased hydrophilicity of the blend nanofibres was found to be responsible for these alterations. Thanks to the presence of chitosan, the interaction with water increases, thus allowing for a significantly faster and more sensitive response. The use of the polymer blend containing chitosan is thus essential for the development of rapid and sensitive pH-sensitive sensors ideally suited for medical applications.

Acknowledgements

The Research Board of Ghent University (BOF) and the Fund for Scientific Research - Flanders (FWO) are acknowledged for their financial support.

Figure captions

Figure 1. SEM images of PCL blank nanofibres (a), PCL 0.5 % omf NY nanofibres (b), PCL 0.5 % omf NY, 4 % omf complexing agent nanofibres (c), PCL/chitosan blank nanofibres (d), PCL/chitosan 0.5 % omf NY nanofibres (f), PCL/chitosan 0.5 % omf NY, 4 % omf complexing agent nanofibres (g)

Figure 2. DVS measurement of PCL(■) and PCL/chitosan (●) nanofibrous structure

Figure 3. Normalised absorbance of NY in aqueous solutions (a), normalised Kubelka-Munk value of PCL nanofibrous structures with 0.25 and 1 % omf NY and 4 % omf complexing agent (b), normalised Kubelka-Munk value of PCL/chitosan nanofibrous structure with 0.25 and 1 % omf NY and 4 % omf complexing agent (c), normalised Kubelka-Munk value of PCL nanofibrous structure with 0.25 and 1 % omf NY and 4 % omf complexing agent after 24 h (d).

Figure 4. Normalised Kubelka-Munk of PCL/chitosan (black), PCL recorded after 3h (grey) and after 24h (grey, dashed) with 0.5 % omf NY and 4 % omf complexing agent at pH 6

Figure 5. Structural formulas of NY (a), PCL (b), chitosan (c) and model compounds for PCL (d) and chitosan (e).

Figure 6. Optimised structures of the NY-PCL complexes (M06-2X/6-311G(d,p)).

Figure 7. Optimised structures of the NY-chitosan complexes (M06-2X/6-311G(d,p)).

References

Bhattarai, N., Li, Z., Gunn, J., Leung, M., Cooper, A., Edmondson, D., Veiseh, O., Chen, M.H., Zhang, Y., Ellenbogen, R.G., & Zhang M. (2009). Natural-Synthetic Polyblend Nanofibers for Biomedical Applications. *Advanced Materials*, 21, 2792-2797.

Braier, N.C., & Jishi, R.A. (2000). Density functional studies of Cu2+ and Ni2+ binding to chitosan. *Journal Of Molecular Structure-Theochem*, 499, 51-55.

Catak, S., D'hooghe, M., De Kimpe, N., Waroquier, M., & Van Speybroeck, V. (2010). Intramolecular π-π Stacking Interactions in 2-Substituted N,N-Dibenzylaziridinium Ions and Their Regioselectivity in Nucleophilic Ring-Opening Reactions. *Journal of Organic Chemistry*, 75, 885-896.

Catak, S., Hemelsoet, K., Hermosilla, L., Waroquier, M., & Van Speybroeck, V. (2011). Competitive Reactions of Organophosphorus Radicals on Coke Surfaces. *Chemistry - A European Journal*, 17, 12027-12036.

Cooper, A., Bhattarai, N., & Zhang, M. (2011b). Fabrication and cellular compatibility of aligned chitosan–PCL fibers for nerve tissue regeneration. *Carbohydrate Polymers*, 85, 149-156.

De Meyer, T., Hemelsoet, K., Van der Schueren, L., Pauwels, E., De Clerck, K., & Van Speybroeck, V. (2012). The halochromic properties of azo dyes in aqueous environment using a combined experimental and theoretical approach. *Chemistry – A European Journal* (in press, DOI: 10.1002/chem.201103633).

Ertekin, K., Karapire, C., Alp, S., Yenigul, B., & Icli, S. (2003). Photophysical and photochemical characteristics of an azlactone dye in sol-gel matrix; a new fluorescent pH-indicator. *Dyes and Pigments*, 56, 125-133.

Fengyu, L., Yong, Z., Sen, W., Dong, H., Lei, J., & Yanlin, S. (2009). Thermochromic core-shell nanofibers fabricated by melt coaxial electrospinning. *Journal of Applied Polymer Science*, 112, 269-274.

Frisch, M.J., Trucks, G.W., Schlegel, H.B., Scuseria, G.E., Robb, M.A., Cheeseman, J.R., Scalmani, G., Barone, V., Mennucci, B., Petersson, G.A., Nakatsuji, H., Caricato, M., Li, X., Hratchian, H.P., Izmaylov, A.F., Bloino, J., Zheng, G., Sonnenberg, J.L., Hada, M., Ehara, M., Toyota, K., Fukuda, R., Hasegawa, J., Ishida, M., Nakajima, T., Honda, Y, Kitao, O., Nakai, H., Vreven, T., Montgomery, Jr., J.A., Peralta, J.E., Ogliaro, F., Bearpark, M., Heyd, J.J., Brothers, E., Kudin, K.N., Staroverov, V.N., Kobayashi, R., Normand, J., Raghavachari, K., Rendell, A., Burant, J.C., Iyengar, S.S., Tomasi, J., Cossi, M., Rega, N., Millam, N.J.,

Klene, M., Knox, J.E., Cross, J.B., Bakken, V., Adamo, C., Jaramillo, J., Gomperts, R., Stratmann, R.E., Yazyev, O., Austin, A.J., Cammi, R., Pomelli, C., Ochterski, J.W., Martin, R.L., Morokuma, K., Zakrzewski, V.G., Voth, G.A., Salvador, P., Dannenberg, J.J., Dapprich, S., Daniels, A.D., Farkas, Ö., Foresman, J.B., Ortiz, J.V., Cioslowski, J., & Fox, D.J. (2009). Gaussian 09, Revision A.1. Gaussian, Inc., Wallingford CT.

Garcia-Heras, M., Gil, C., Carmona, N., Faber, J., Kromka, K., & Villegas, M.A. (2005). Optical behaviour of pH detectors based on sol-gel technology. *Analytica Chimica Acta*, 540, 147-152.

Greiner, A., & Wendorff, J.H. (2007). Electrospinning: A Fascinating Method for the Preparation of Ultrathin Fibers. *Angewandte Chemie*, 46, 5670-5703.

Gu, J. D., Wang J., Leszczynski, J., Xie, Y. M., & Schaefer, H. F. (2008). To stack or not to stack: Performance of a new density functional for the uracil and thymine dimers. *Chemical Physics Letters*, 459, 164-166.

Hong, S., & Kim, G. (2011). Fabrication of electrospun polycaprolactone biocomposites reinforced with chitosan for the proliferation of mesenchymal stem cells. *Carbohydrate Polymers*, 83, 940-946.

Jacquemin, D., Preat, J., Perpète, E.A., Vercauteren, D.P., André, J.M., Ciofini, I., & Adamo, C. (2010). Absorption spectra of azobenzenes simulated with time-dependent density functional theory. *International Journal of Quantum Chemistry*, 111, 4224-4240.

Jurmanovic, S., Kordic, S., Steinberg, M.D., & Steinberg, M.I. (2010). Organically modified silicate thin films doped with colourimetric pH-indicators methyl red and bromocresol green as pH-responsive solegel hybrid materials. *Thin Solid Films*, 518, 2234-2240.

Li, D., & Xia, J. (2004). Electrospinning of nanofibers: reinventing the wheel. *Advanced Materials*, 16, 1151-1170.

Little, A.F., & Christie, R.M. (2010). Textile applications of photochromic dyes. Part 1: establishment of a methodology for evaluation of photochromic textiles using traditional colour measurement instrumentation. *Coloration Technology*, 126, 157-163.

Liu, S.P., Tan, L.J., Hu, W.L., Li, X.Q., & Chen, Y.M. (2010) Cellulose acetate nanofibers with photochromic property: Fabrication and characterization. *Materials Letters*, 64, 2427-2430.

Lloyd, L.L., Kennedy, J.F., Methacanon, P., Paterson, M., & Knill, C.J. (1998). Carbohydrate polymers as wound management aids. *Carbohydrate Polymers*, 37, 315-322.

Malherbe, I., Sanderson, R.D., & Smit, E. (2010). Reversibly thermochromic micro-fibres by coaxial electrospinning. *Polymer*, 51, 5037-5043.

578 Mao, W., Vail, S.A., Keirstead, A.E., Marquez, M., Gust, D., & Garcia, A.A. (2009).
579 Preparation of photochromic poly(vinylidene fluoride-co-hexafluoropropylene) fibers by
580 electrospinning. *Polymer*, 50, 2974-2980.
581 Markova, N., Sparr, E., & Wadso, L. (2001). On application of an isothermal sorption
582 microcalorimeter. *Thermochimica Acta*, 374, 93-104.
583 Matilla, H.R. (2006). *Intelligent Textiles and Clothing*. Cambridge:Woodhead, (Part 3).
584 Ramakrishna, S., Fujihara K., Teo, W.E., Lim, T.C., & Ma, Z. (2005). *Electrospinning and*
585 *nanofibres*. (1th ed.). Singapore:World Scientific, (Chapter 2).
586 Moghe, A.K., Hufenus, R., Hudson, S.M., & Gupta, B.S. (2009). Effect of the addition of a
587 fugitive salt on electrospinnability of poly(ε-caprolactone). *Polymer*, 50, 3311-3318.
588 Prabhakaran, M.P., Venugopal, J.R., Chyan, T.T., Hai, L.B., Chan, C.K., Lim, A.Y., &
589 Ramakrishna, S. (2008) Electrospun biocomposite nanofibrous scaffolds for neural tissue
590 engineering. *Tissue Engineering Part A*, 14, 1787-1797.
591 Sangwichien, C., Aranovich, G.L. & Donohue, M.D. (2002). Density functional theory
592 predictions of adsorption isotherms with hysteresis loops. *Colloids and Surfaces A:*
593 *Physicochemical and Engineering Aspects*, 206, 313–320.
594 Stuart, M.A.C., Huck, W.T.S., Genzer, J., Muller, M., Ober, C., Stamm, M., Sukhorukov,
595 G.B., Szleifer, I., Tsukruk, V.V., Urban, M., Winnik, F., Zauscher, S., Luzinov, I., & Minko,
596 S. (2010). Emerging applications of stimuli-responsive polymer materials. *Nature Materials*,
597 9, 101-113.
598 Teimouri, A., Chermahini, A.N., Taban, K., & Dabbagh, H.A. (2009). Experimental and CIS,
599 TD-DFT, ab initio calculations of visible spectra and the vibrational frequencies of sulfonyl
600 azide-azoic dyes.. *Spectrochimica Acta Part A - Molecular and Biomolecular Spectroscopy*,
601 72, 369-377.
602 Van der Schueren, L., & De Clerck, K. (2010a). The use of pH-indicator dyes for pH-
603 sensitive textile materials. *Textile Research Journal*, 80, 590-603.
604 Van der Schueren, L., Mollet, T., Ceylan, Ö., & De Clerck, K. (2010b). The development of
605 polyamide 6.6 nanofibres with a pH-sensitive function by electrospinning. *European Polymer*
606 *Journal*, 46, 2229-2239.
607 Van der Schueren, L., De Schoenmaker, B., Kalaoglu, O.I., & De Clerck, K. (2011). An
608 alternative solvent system for the steady state electrospinning of polycaprolactone. *European*
609 *Polymer Journal*, 47, 1256-1263.

Van der Schueren, L., & De Clerck, K. (2012a). Coloration and application of pH-sensitive dyes on textile materials. *Coloration Technology*, 128, 1-9.

Van der Schueren, L., Steyaert, I., De Schoenmaker, B., & De Clerck, K. (2012b). Polycaprolactone/chitosan blend nanofibres electrospun from an acetic acid/formic acid solvent system. *Carbohydrate Polymers*, 88, 1221-1226.

Van der Schueren, L., Hemelsoet, K., Van Speybroeck, V., & De Clerck, K. (2012c). The influence of a polyamide matrix on the halochromic behaviour of the pH-sensitive azo dye Nitrazine Yellow. *Dyes and Pigments*, 94, 443-451.

Yang, H., Chen, X., & Wang, H. (2009). Acceleration of osteogenic differentiation of preosteoblastic cells by chitosan containing nanofibrous scaffolds. *Biomacromolecules*, 10, 2772-2778.

Zhao, Y., & Truhlar, D.G. (2008). The M06 suite of density functionals for main group thermochemistry, thermochemical kinetics, noncovalent interactions, excited states, and transition elements: two new functionals and systematic testing of four M06-class functionals and 12 other functionals. *Theoretical Chemical Accounts*, 120, 215-241.

Table 1

Table 1. Conductivity, average fibre diameter and dye release of PCL and PCL/chitosan solutions as a function of the NY concentration and presence of complexing agent (CA)

		PCL			*PCL/chitosan*		
% omf NY	*% omf CA*	*Conductivity (mS/cm)*	*Fibre diameter (nm)*	*Dye release (%)*	*Conductivity (mS/cm)*	*Fibre diameter (nm)*	*Dye release (%)*
0	0	0.089	364 ± 83	/	0.888	196 ± 46	/
0.5	0	0.216	337 ± 53	4.8	0.928	183 ± 45	57.1
0.25	4	0.480	310 ± 55	0.0	1.239	167 ± 47	0.0
0.5	4	0.502	343 ± 45	0.0	1.250	168 ± 43	0.0
1	4	0.530	374 ± 71	1.2	1.280	184 ± 48	7.1

Figure 1

Click here to download high resolution image

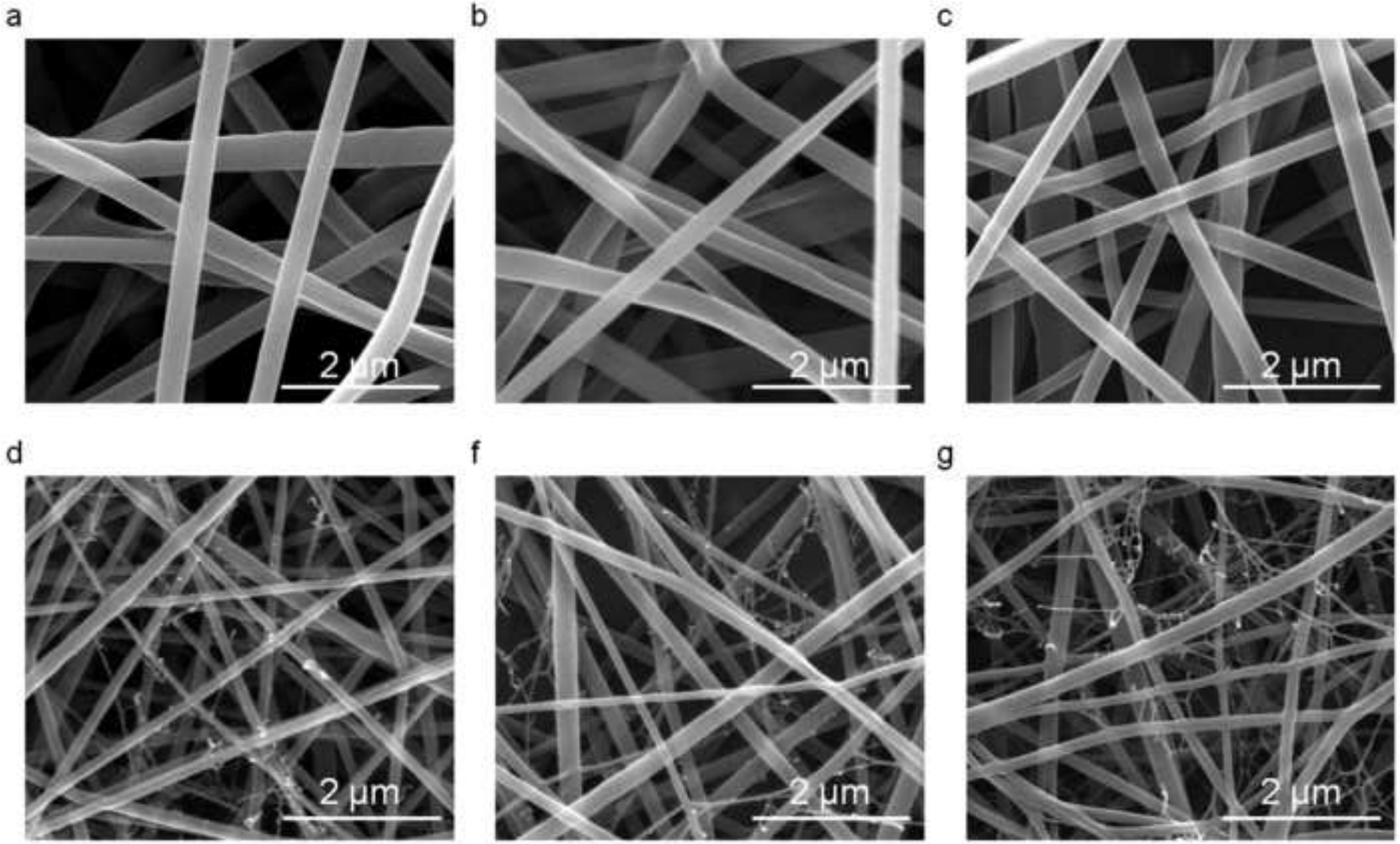

Figure 2

Click here to download high resolution image

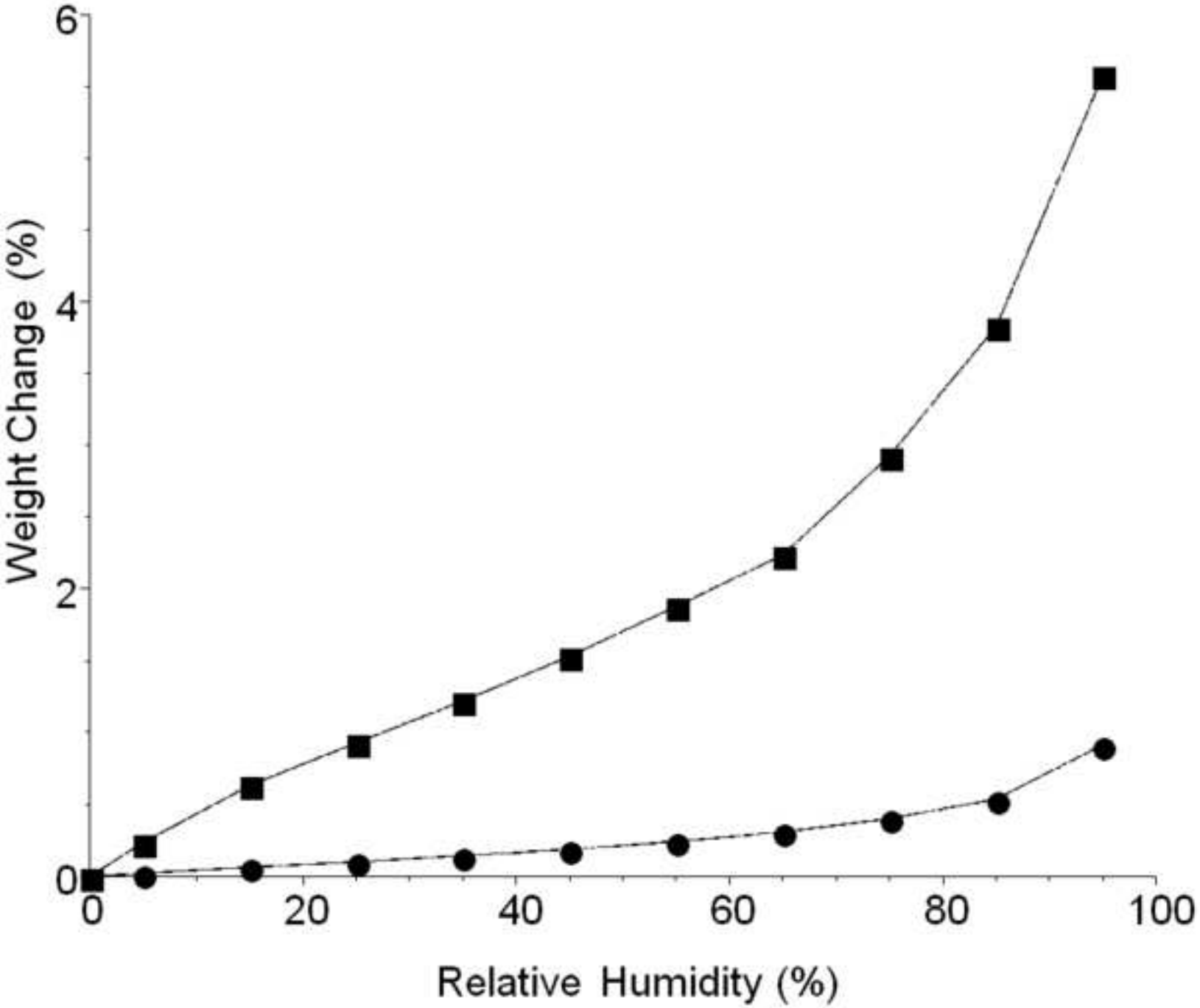

Figure 3

Click here to download high resolution image

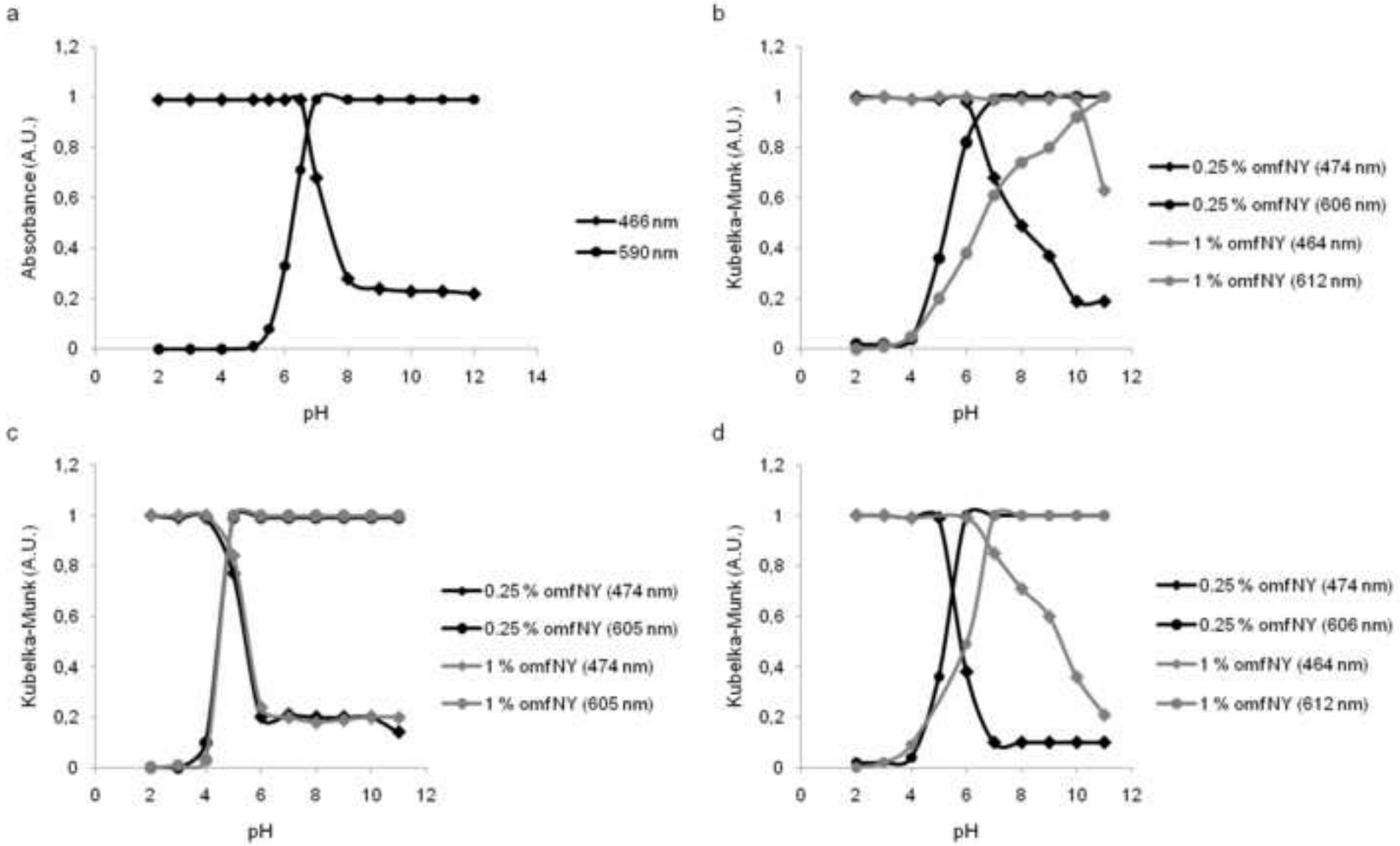

Figure 4

Click here to download high resolution image

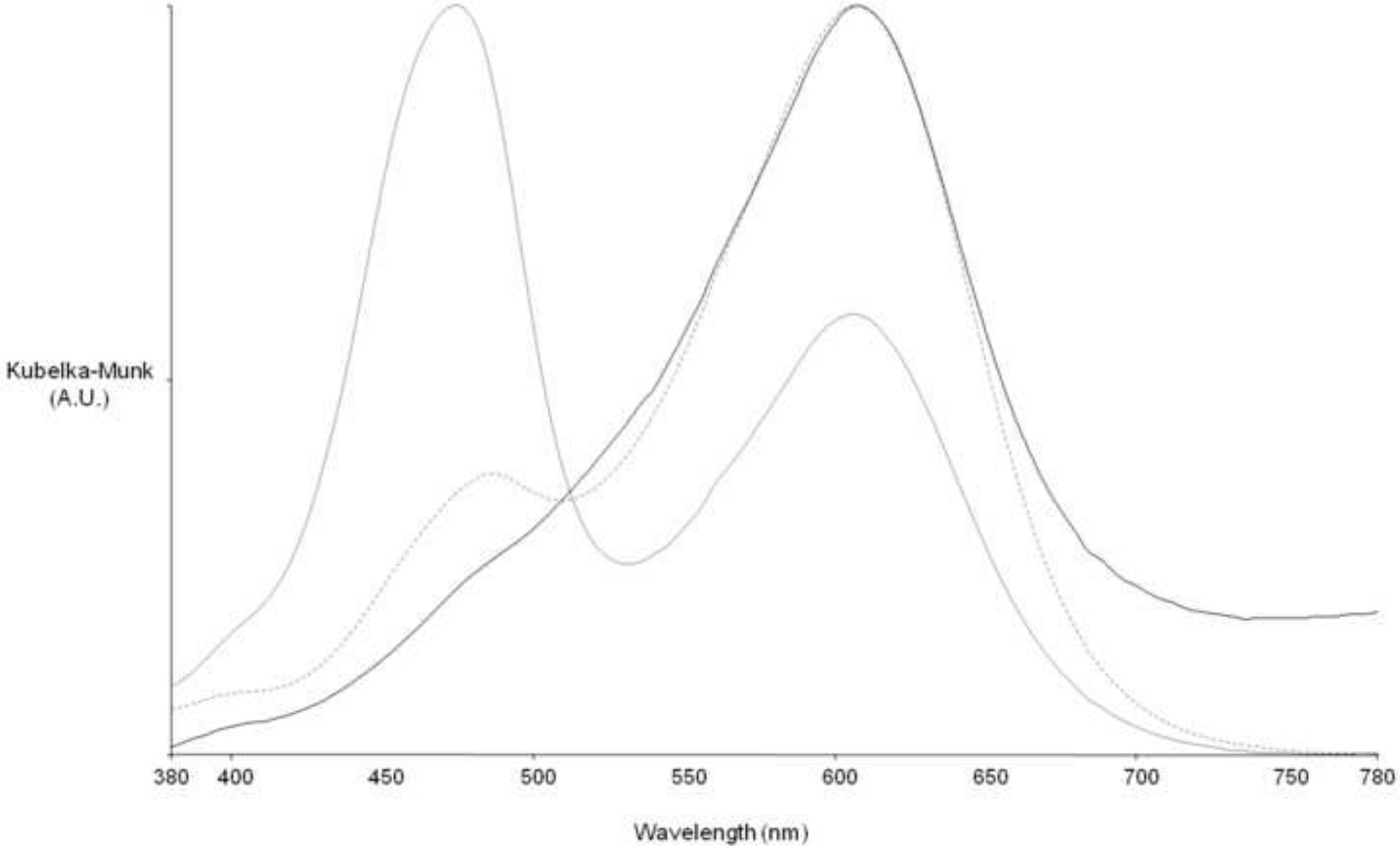

Figure 5

Click here to download high resolution image

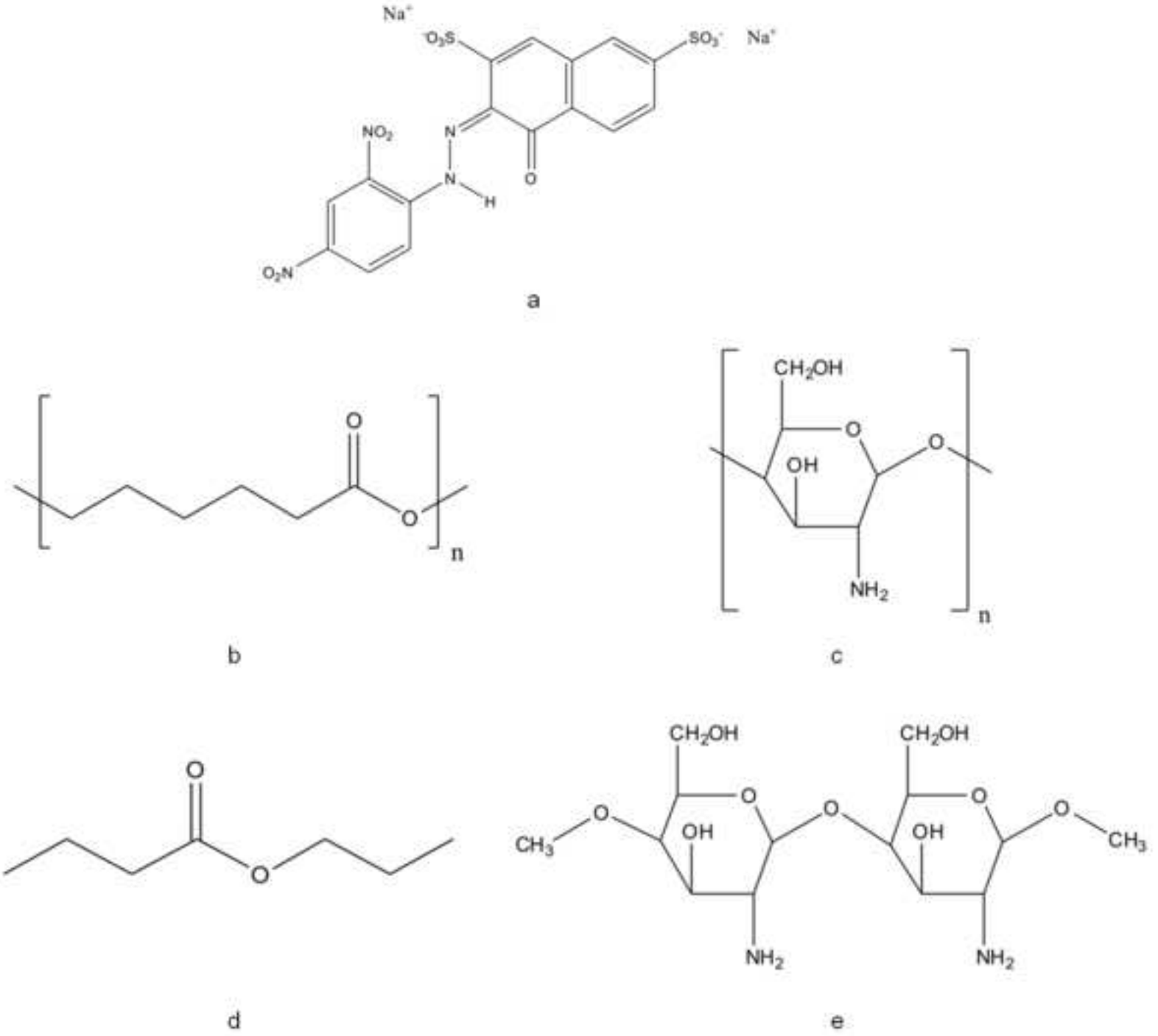

Figure 6

Click here to download high resolution image

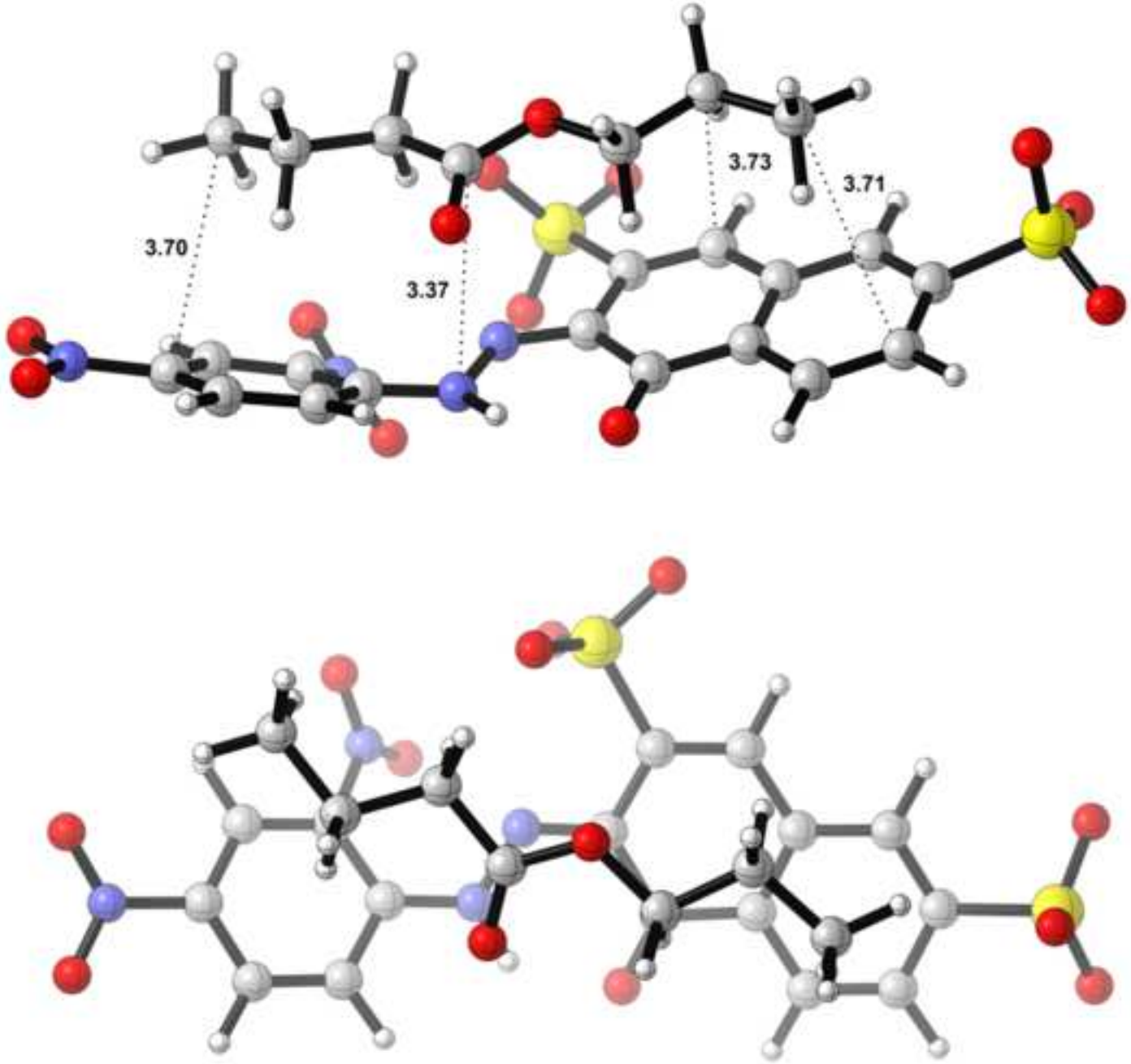

Figure 7

Click here to download high resolution image